



A *Phytophthora* effector protein promotes symplastic cell-to-cell trafficking by physical interaction with plasmodesmata-localised callose synthases

Iga Tomczynska^{1,2} , Michael Stumpe¹, Tu Giang Doan¹ and Felix Mauch¹ 

¹Department of Biology, University of Fribourg, 1700 Fribourg, Switzerland; ²Present address: Department of Botany and Plant Pathology, Oregon State University, Corvallis, OR 97331-8530, USA

Author for correspondence:

Iga Tomczynska

Tel: +1 541 737 3679

Email: tomczyni@oregonstate.edu

Received: 10 December 2019

Accepted: 20 April 2020

New Phytologist (2020)

doi: 10.1111/nph.16653

Key words: Arabidopsis, callose, callose synthase, *Nicotiana benthamiana*, *Phytophthora*, plant immunity, plasmodesmata, RxLR effector.

Summary

- Pathogen effectors act as disease promoting factors that target specific host proteins with roles in plant immunity. Here, we investigated the function of the RxLR3 effector of the plant-pathogen *Phytophthora brassicae*.
- Arabidopsis plants expressing a FLAG-RxLR3 fusion protein were used for co-immunoprecipitation followed by liquid chromatography-tandem mass spectrometry to identify host targets of RxLR3. Fluorescently labelled fusion proteins were used for analysis of subcellular localisation and function of RxLR3.
- Three closely related members of the callose synthase family, CalS1, CalS2 and CalS3, were identified as targets of RxLR3. RxLR3 co-localised with the plasmodesmal marker protein PDL5 (PLASMODESMATA-LOCALISED PROTEIN 5) and with plasmodesmata-associated deposits of the β -1,3-glucan polymer callose. In line with a function as an inhibitor of plasmodesmal callose synthases (CalS) enzymes, callose depositions were reduced and cell-to-cell trafficking was promoted in the presence of RxLR3.
- Plasmodesmal callose deposition in response to infection was compared with wild-type suppressed in RxLR3-expressing Arabidopsis lines. Our results implied a virulence function of the RxLR3 effector as a positive regulator of plasmodesmata transport and provided evidence for competition between *P. brassicae* and Arabidopsis for control of cell-to-cell trafficking.

Introduction

Symplastic cell-to-cell channels called plasmodesmata (PD) are unique features of higher plants. They bridge the rigid plant cell wall to connect adjacent cells. Nearly all cells of a plant are connected via PD into a symplastic continuum (Gunning & Robards, 1976; Roberts & Oparka, 2003). PD serve as transport routes to the vascular system and play diverse roles in coordination at the cellular and organism level. PD pores are lined with a plasma membrane that is continuous between adjacent cells. Similarly, the endoplasmic reticulum (ER) is connected through PD and becomes tightly compressed into a central rod, called a desmotubule. Many proteins have been identified in PD proteomes (Fernandez-Calvino *et al.*, 2011; Bayer & Salmon, 2013; Grison *et al.*, 2015). However, only relatively few proteins have been proven experimentally to be associated with PD (Faulkner & Maule, 2011). PD accumulate deposits of the β -1,3-glucan polymer callose at both ends of the PD channel. The callose collar is one of the determinants of the size exclusion limit (SEL), which is defined by the largest molecule that can pass through the channel (Zavaliev *et al.*, 2011). Intercellular trafficking through PD includes transport of small molecules such as nutrients, metabolites, hormones and other signalling molecules. In

addition, PD enable cell-to-cell trafficking of macromolecules including proteins and nucleic acids (Lucas *et al.*, 1995; Oparka, 2004; Reagan *et al.*, 2018). Many of these macromolecules have noncell autonomous functions, emphasising the importance of PD in cell-to-cell communication (Lucas *et al.*, 1995; Nakajima *et al.*, 2001; Seville *et al.*, 2015; Cheval & Faulkner, 2018).

Plants can dynamically control symplastic connectivity by modulating the SEL of PD. The callose depositions around PD openings play a major role in this process (Radford *et al.*, 1998; Roberts & Oparka, 2003). The amount of callose deposited at PD is the result of the balanced activities of two antagonistic groups of enzymes, CalS and callose degrading β -1,3-glucanases (Vatén *et al.*, 2011; Zavaliev *et al.*, 2011; De Storme & Geelen, 2014; Amsbury *et al.*, 2017). Callose synthases (CalS) are encoded by a multigene family and utilise UDP-glucose as a substrate to synthesise and transfer callose across the plasma membrane to the apoplast. The active enzymes are part of a complex with other proteins some of which have regulatory functions (Verma & Hong, 2001; De Storme & Geelen, 2014). Individual CalS have defined roles in the formation of cell plates during cell division, during pollen tube and gametophyte development, in sieve plate formation and in the deposition of local cell wall reinforcements at sites of attempted pathogen penetration (Chen

& Kim, 2009; Nedukha, 2015). In *Arabidopsis*, four CalS have been implicated in the regulation of PD. They include CalS1 (also named GLUCAN SYNTHASE-LIKE 6; GSL6), CalS3 (GSL12), CalS8 (GSL4) and CalS10 (GSL8) (Guseman *et al.*, 2010; Vatén *et al.*, 2011; Han *et al.*, 2014; Cui & Lee, 2016). Plant β -1,3-glucanases belong to a large protein family. In *Arabidopsis* three β -1,3-glucanases were shown to play a role in plasmodesmal callose degradation (Benitez-Alfonso *et al.*, 2013).

PD have essential roles in plant defence against microbial pathogens. The best-known example is the systemic PD-mediated spread of viruses (Benitez-Alfonso *et al.*, 2010). PD are important for nutritional sink–source relationships, the systemic spread of signalling molecules in systemic acquired resistance (SAR) and in the systemic spread of immune-relevant small molecules (Lim *et al.*, 2016; Cheval & Faulkner, 2018). Interestingly, pathogen-produced effector proteins can also spread via PD into cells adjacent to infection sites (Kankanala *et al.*, 2007; Cao *et al.*, 2018). Pathogen effectors subvert host immunity or alter cellular homeostasis with the aim to reduce disease resistance (Giraldo & Valent, 2013). With few exceptions, this goal is achieved by binding to specific host target proteins to inhibit their function. Trafficking through PD suggests that some effectors might prepare host cells for an upcoming invasion (Khang *et al.*, 2010). One of the best analysed groups of effectors of filamentous pathogens are the RxLR effectors of oomycetes (Whisson *et al.*, 2011; Anderson *et al.*, 2015). This class of organisms includes downy mildews and the genus *Phytophthora*, with *P. infestans* responsible for the late blight disease of potato and tomato and *P. sojae* causing stem and root rot in soybeans. RxLR effectors are named based on a conserved RxLR amino acid motif (Arg–any amino acid–Leu–Arg) downstream of a secretory signal peptide. The RxLR motif is thought to be required for effector translocation into host cells (Whisson *et al.*, 2007), but the mechanism of translocation is under debate (Kale *et al.*, 2010; Tyler *et al.*, 2013; Petre *et al.*, 2016; Wawra *et al.*, 2017). Recent evidence has suggested that the RxLR motif may function as an internal sorting signal that is cleaved before secretion (Wawra *et al.*, 2017). The sequence responsible for the actual virulence function is encoded by the C-terminal part that follows the RxLR motif. Individual oomycete species can produce hundreds of different RxLR effectors (Haas *et al.*, 2009; Tyler, 2009). Some host targets of RxLR effectors have been identified in recent years and, in line with their virulence function, their ectopic expression in host plants usually enhanced disease susceptibility (Anderson *et al.*, 2015). Some examples include RxLR effectors that interact with components of immune-associated protein kinase signalling (King *et al.*, 2014; Zheng *et al.*, 2014; Murphy *et al.*, 2018) or vesicle trafficking (Chaparro-Garcia *et al.*, 2015; Du *et al.*, 2015; Tomczynska *et al.*, 2018), whereas others interact with less obvious targets involved in RNA splicing (Huang *et al.*, 2017), small RNA biogenesis (Qiao *et al.*, 2015), histone acetylation (Kong *et al.*, 2017), autophagy (Dagdas *et al.*, 2016) and ER stress-mediated immunity (Jing *et al.*, 2016; Fan *et al.*, 2018).

Here, we analyse the virulence function of the RxLR3 effector (RxLR3) of *Phytophthora brassicae* that can infect plants belonging to the Brassicaceae family, including different varieties of

Brassica oleracea and *Arabidopsis*. We present evidence that RxLR3 localises to PD and physically interacts with CalS that control trafficking through PD. RxLR3 inhibits callose accumulation at PD and promotes PD-dependent cell-to-cell trafficking.

Materials and Methods

Biological material

Nicotiana benthamiana plants were grown under a 16 h : 8 h, light : dark, 28°C : 25°C cycle. *Arabidopsis* plants were cultivated using a 12 h : 12 h, light : dark, 21°C : 19°C cycle. For tests of disease resistance, the adaxial leaf surface of 3-wk-old *Arabidopsis* plants was inoculated with 30- μ l droplets of a zoospore suspension (10^5 zoospores ml^{-1}) of the *P. brassicae* isolate CBS 179.87 (Roetschi *et al.*, 2001). Disease resistance was evaluated based on lesion size according to a previously described scale (Schlaeppli *et al.*, 2010). The kinetics of expression of RxLR3 during the infection process was analysed by qPCR in the susceptible *Arabidopsis* mutant *cyp79B2cyp79B3* inoculated with zoospores of *P. brassicae* isolate CBS179.87.

Cloning and bacterial transformation

Information about gene-specific primers, cDNAs, destination vectors and final fusion proteins is summarised in Supporting Information Tables S1, S2. PCR amplifications were performed using Phusion High-Fidelity DNA Polymerase (New England Biolabs, Allschwil, Switzerland). The amplification products were cloned into pENTR (pENTR/D-TOPO Cloning; Invitrogen) and transformed into *Escherichia coli* XL1 Blue cells. Following sequence verification, cDNA inserts were mobilised into Gateway destination vectors to be used for transformation of *Agrobacterium tumefaciens* strain GV3101 using the freeze–thaw method (Schütze *et al.*, 2009).

Transformation of *Arabidopsis*

Arabidopsis plants were transformed by the floral dip method (Clough & Bent, 1998) with *agrobacteria* containing the FLAG-RxLR3 construct cloned into the binary vector pFASTG02 (Shimada *et al.*, 2010). Transformed plants were selected based on green fluorescence emission in the seeds or by screening with BASTA. Transformants were tested for transgene expression by qPCR analysis and immunoblotting following standard procedures. Homozygous FLAG-RxLR3 lines carrying one copy of the transgene were selected based on segregation analysis.

Agroinfiltration of *N. benthamiana*

Agrobacterium tumefaciens strain GV3101 was used for agroinfiltration experiments as described (Schütze *et al.*, 2009). Leaves of 3–4-wk-old *N. benthamiana* plants were infiltrated with a 1 : 1 mixture of *Agrobacterium* containing the respective constructs and a P19 silencing suppressor strain. The concentration of *Agrobacterium* suspensions used for agroinfiltration was adjusted depending on the experiment. A suspension with an OD₆₀₀ of

0.1 was used for localisation experiments. To achieve expression in large clusters of epidermal cells the OD₆₀₀ was adjusted to 0.15. For restricted expression in a few cells the OD₆₀₀ was adjusted to an OD of 0.0005.

Immunoprecipitation and MS analysis

Untargeted co-immunoprecipitation (Co-IP) experiments were based on FLAG-tagged RxLR3 constructs and included as negative controls FLAG-tagged versions of three unrelated RxLR effector proteins of *P. brassicae* (Table S3). Leaves of 5-wk-old Arabidopsis plants expressing tagged effector proteins were frozen in liquid nitrogen and ground to a fine powder. Co-IP was performed and analysed as described (Tomczynska *et al.*, 2018). For verification of effector–target interaction, a green fluorescent protein (GFP)-tagged version of CalS3 (GFP-CalS3; (Vatén *et al.*, 2011) or free GFP as a negative control was expressed in agroinfiltrated leaves of *N. benthamiana* together with FLAG-RxLR3. Co-IP conditions were as described previously (Tomczynska *et al.*, 2018). Here, 2 g of tissue was used with a 3 h incubation period at 4°C with agarose beads coupled to an anti-GFP antibody (GFP-Trap[®] A; Chromotek GmbH, Planegg-Martinsried, Germany) to immunoprecipitate GFP-CalS3 or free GFP. The samples were processed as described by the manufacturer. After the final washing step, the proteins attached to the agarose beads were solubilised in 50 µl of SDS sample buffer and 25 µl aliquots were analysed by SDS–PAGE and immunoblotting.

Protein analysis

SDS–PAGE and immunoblotting were performed with standard procedures. FLAG-tagged proteins were detected with a monoclonal anti-FLAG M2-peroxidase antibody (Sigma). Anti-GFP antibody conjugated with horseradish peroxidase (HRP) (Santa Cruz Biotechnology, Heidelberg, Germany) was used for detection of GFP.

RNA extraction, cDNA synthesis and qPCR

Total RNA was extracted using the Spectrum Plant Total RNA Kit (Sigma). Here, 2 µg of total RNA were used for cDNA synthesis (Omniscript Reverse Transcription Kit; Qiagen). The mix for qPCR reactions contained 7.5 µl of SYBR Green (Bioline), cDNA (corresponding to 100 ng RNA) and primers at a concentration of 10 µM in a final volume of 15 µl. Runs were performed on a Mic qPCR machine (Bio Molecular Systems, Chatel-St-Denis, Switzerland). The final PCR products were analysed by melting point analysis.

Plasmodesmal callose staining and quantification in uninfected tissues

Callose depositions were stained with aniline blue infiltrated into leaves of Arabidopsis or *N. benthamiana* as described previously (Gaudioso-Pedraza & Benitez-Alfonso, 2014). Three-wk-old Arabidopsis plants were used and one leaf per plant (the fourth leaf in the rosette counting from the oldest) was stained. A single

experiment included three leaves (from three plants), seven photographs from the central part of the leaf were taken from each. A single experiment for 3–4-wk-old *N. benthamiana* plants consisted of three plants (one fully developed leaf per plant). For each leaf two squares (1 cm² each) from the central part of the leaf (from both sides of the vein) were collected and eight photographs from each square were taken. Callose staining on the abaxial site of leaves was detected using a Visitron VisiScope CSU-W1 confocal microscope and an excitation wavelength of 405 nm (120 mW) and an emission wavelength of 460/50 nm. IMAGEJ software (<https://imagej.net>) was used for quantification of callose signal intensity (Zavaliev & Epel, 2015). Quantification was based on photographs collected in two independent experiments.

Analysis of plasmodesmal callose deposition after *P. brassicae* infection

The experiment was performed on 3-wk-old Arabidopsis plant leaves. The abaxial side of detached leaf (one leaf/plant) was inoculated with a 10-µl droplet of *P. brassicae* zoospore suspension (50 000 zoospores ml^{−1}) and placed in high humidity and darkness at 18°C. PD callose staining was performed 6 hai and scoring was visualised using a confocal microscope 7 hai. The experiment was performed twice, in each test four leaves per genotype were used and five cells challenged by zoospore penetration per leaf were scored. Numbers of callose induction events were based on a comparison of callose staining in invaded cells vs neighbouring cells as the reference. To standardise the method the following criteria were used:

- (1) The cell was considered as invaded if the *P. brassicae* cyst formed an appressorial germination tube that tried to penetrate that cell.
- (2) The cells penetrated by more than one zoospore were excluded.
- (3) In case of anticlinal penetration when there was a risk that the neighbouring cell was also affected, the neighbouring cell was excluded as the reference.
- (4) Quantification of PD callose induction was based on assessment on five different areas covering the plasma membranes of the invaded cell and its neighbouring cells.
- (5) Within the single area (of size at least 25 × 50 µm) PD callose was considered as induced if: (i) at least four PD callose spots were visible, and (ii) at least 50% of PD callose deposits in the invaded cell showed a double diameter visible to the naked eye in comparison with the PD callose in the area of the neighbouring cells.
- (6) If it showed no obvious difference – the area was considered as the area with no-induction event. If at least three out of five areas showed induction events – the invaded cell was scored as the one with induced PD callose deposition.

Analysis of PD conductivity

Analysis of PD conductivity based on the cell-to-cell movement of a GFP tracer was performed essentially as described (Stonebloom *et al.*, 2009; Burch-Smith & Zambryski, 2010)

with a minor modification. *A. tumefaciens* strain GV3101 was co-transformed with cyan fluorescent protein (CFP) containing an ER-retention signal as a marker of transformed cells (ER-CFP in CD3-742 carrying a kanamycin resistance gene) and free GFP as a mobile fluorescent tracer (GFP in pB7WGF2, spectinomycin resistance). Co-transformed agrobacteria were selected on medium containing rifampicin, gentamycin, spectinomycin and kanamycin. Two leaves of two *N. benthamiana* plants were infiltrated with combinations of agrobacteria containing the GFP tracer and the ER-CFP construct (final OD₆₀₀ of 0.0005), the P19 silencing construct (final OD₆₀₀ of 0.15) and the FLAG-RxLR3 construct (final OD₆₀₀ of 0.15). At 48 h after agroinfiltration, each leaf was divided into two halves: one half stayed on the plant as a control and the second half was removed from the plant and treated with salicylic acid (SA; Zavaliev & Epel, 2015). The abaxial side was sprayed with 5 mM SA and leaves were placed in darkness for 24 h under high humidity conditions before analysis. The distribution of ER-CFP and the GFP tracer was observed 72 h post agroinfiltration by confocal microscopy. Results were based on two independent experiments with a total number of foci per treatment of $n = 176$.

Confocal microscopy and image processing

Confocal images were made using an inverted Spinning Disk Confocal Microscope, VisiScope CSU-W1, equipped with an Evolve 512 EM-CDD camera (Photometrics) and a Scientific Grade 4.2 sCMOS camera. The following excitation wavelengths were used for detection of fluorescence tags: 488 nm (200 mW) for GFP; 515 nm (100 mW) for red fluorescent protein (RFP), 561 nm (200 mW) for mCherry, 445 nm (100 mW) for CFP and 488 nm (200 mW) for yellow fluorescent protein (YFP). The single emission bands were for GFP at 525/50 nm, for RFP 575LP, for mCherry at 609/57 nm, for CFP at 470/24 nm and for YFP at 535/30 nm. Images were projected and processed using IMAGEJ software (<https://imagej.net>). Photographs with enhanced resolution were obtained at the BioImaging and Optics Core Facility, EPFL, Lausanne, Switzerland, using a Confocal LSM710 microscope (Zeiss) equipped with BiG detector, and the oil objective Plan-Apochromat 63×/1.40. For this objective, the technical shift (measured) for red and green channels was below 40 nm. Wavelengths for YFP and mCherry detection were 458 nm and 561 nm, respectively.

Results

Characterisation of the RxLR3 effector of *P. brassicae*

RxLR3 in *P. brassicae* was discovered in a cDNA and in a genomic library as an intronless gene encoding a protein of 160 amino acids with a molecular mass of 18.1 kDa. RxLR3 contains a predicted N-terminal signal peptide followed by an RxLR-deER motif starting at position 49 and a putative functional C-terminal domain (Fig. S1). RxLR3 is a unique protein with no sequence homology beyond the RxLR-deER motif to effectors of

other *Phytophthora* species. Furthermore the signal peptide and the RxLR-deER motif RxLR3 does not contain any known functional protein domains. Analysis by qPCR showed that the RxLR3 effector was expressed constitutively in cysts and in invading hyphae during infection of the susceptible Arabidopsis mutant *cyp79B2cyp79B3* with a maximal relative expression at 12 h post inoculation (hpi) compared with transcript levels of *P. brassicae* actin and tubulin (Fig. S2).

Analysis of transgenic Arabidopsis lines with ectopic expression of RxLR3

RxLR3 with a N-terminal FLAG-tag but lacking the signal peptide was constitutively expressed under the control of the CaMV-35S promoter in the Arabidopsis accession Wassilewskija (Ws-0). High expression of RxLR3 led to developmental abnormalities and reduced growth (Fig. S3a) suggesting an effect of RxLR3 on general plant metabolism and growth control. The severity of the growth phenotype correlated with RxLR3 protein levels (Fig. S3b,c). The effect of RxLR3 expression on disease resistance towards *P. brassicae* was analysed in transgenic lines L7 and L5 with low to intermediate RxLR3 expression levels to reduce secondary effects of stunted growth. In wild-type plants, 55% of the inoculation sites resulted in full resistance (resistance score 4) whereas this number dropped to 32% in line L7 and to 22% in line L5, with a corresponding increase in infection sites with intermediate resistance scores of 3 and 2 (Fig. S4). Line 5 with intermediate RxLR3 expression was more susceptible than line 7 with low RxLR3 expression. No interactions resulting in high susceptibility (resistance scores 1 and 0) were observed in 80 infection sites tested per genotype.

RxLR3 localises to PD

The subcellular distribution of RxLR3 in Arabidopsis was analysed by confocal microscopy in leaves of *N. benthamiana* that transiently expressed a GFP-RxLR3 or YFP-RxLR3 fusion construct under the control of the CaMV-35S promoter. The fusion protein localised to distinct spots lining the cell periphery (Fig. S5). The pattern of staining was reminiscent of the distribution of PD. To test PD localisation of RxLR3, the pattern of accumulation of YFP-RxLR3 was compared with PD-associated deposition of callose that is known to control PD conductivity. Staining of leaf cells with aniline blue revealed a dot-like distribution of callose along the cell periphery that matched the distribution of YFP-RxLR3 (Fig. 1a). To further confirm PD accumulation, YFP-RxLR3 was co-expressed with a mCherry-tagged fusion protein of the PD marker PLASMODESMATA-LOCALISED PROTEIN 5 (PDLP5; Lee *et al.*, 2011). The fluorescence signal of YFP-RxLR3 was associated with the red fluorescence of PDLP5-mCherry, thus confirming PD localisation of RxLR3 (Fig. 1b). Further imaging with higher resolution and magnification verified that at the single spot where they associated, their signals did not overlap perfectly, but rather the PDLP5-mCherry signal was flanked by two YFP-RxLR3 signals (PD pore photograph in Fig. 1b).

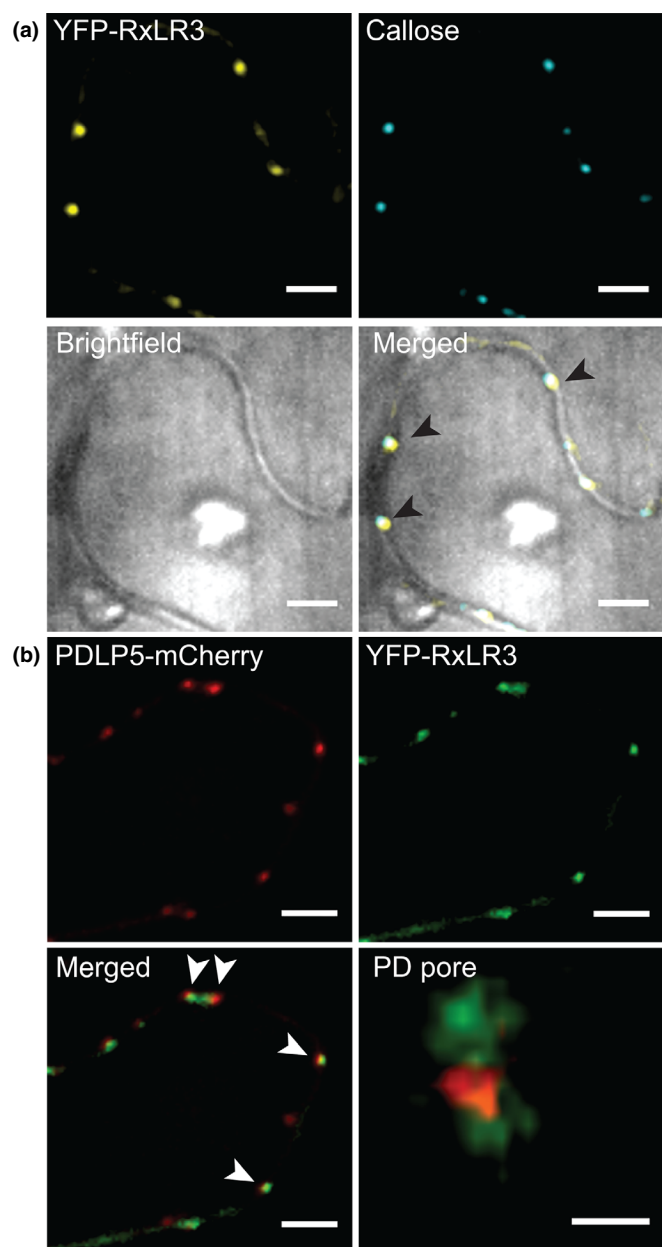


Fig. 1 RxLR3 co-localises with callose deposits and with the plasmodesmata (PD) marker protein PDL5. Fusion constructs were expressed via agroinfiltration in leaves of *Nicotiana benthamiana*. (a) YFP-RxLR3 co-localises with aniline blue-stained callose deposits known to be associated with PD. Examples of co-localisation are marked with arrowheads. Bars, 2 μ m. Each photograph is a z-stack consisting of three images with 1 μ m voxel depth. Photographs were taken 24 h after agroinfiltration. (b) YFP-RxLR3 was co-expressed with PDL5 fused to the red fluorescent protein mCherry. Examples of co-localisation are marked with arrowheads. Each photograph is a z-stack consisting of three images with 0.8 μ m voxel depth. Photographs were taken 24 h after agroinfiltration. Bars, 5 μ m. PD pore is a single photograph of the RxLR3-PDL5 co-localisation spot taken with a Zeiss Plan-Apochromat $\times 63/1.4$ oil objective lens with technical shift below 40 nm. Bar, 0.5 μ m.

RxLR3 targets a subgroup of callose synthases

In planta Co-IP followed by liquid chromatography-tandem mass spectrometry was applied to identify putative host targets of

RxLR3. The FLAG-RxLR3 fusion protein was immunoprecipitated from extracts of transgenic *Arabidopsis* using magnetic beads coated with anti-FLAG antibodies. Mass spectrometry identified four *Arabidopsis* proteins that appeared to exclusively associate with RxLR3 in the immunoprecipitate compared with negative controls and consisting of three unrelated FLAG-RxLR fusion proteins (Table S3). The four proteins all belonged to the CalS (GLUCAN SYNTHASE-LIKE) family. They included CalS3/GSL12 (AT5G13000) with 53 unique peptide matches (including 41 exclusive matches), CalS2/GSL3 (AT2G31960) with 38 unique peptide matches (including 13 exclusive matches) and CalS1/GSL6 (AT1G05570) with 33 unique peptide matches (including nine exclusive matches). CalS5/GSL2 (AT2G13680) was excluded as an RxLR3 effector target as only two unique peptides, but no exclusive match, were present in the co-immunoprecipitate. The next best Co-IP candidates were not further considered as they were also present in immunoprecipitates of the three unrelated RxLR effector controls.

Reciprocal Co-IP was performed with extracts of agroinfiltrated *N. benthamiana* expressing GFP-CalS3 and FLAG-RxLR3. GFP-CalS3 was expressed at a low level and was not detectable in the initial extract (Fig. 2a). However, after concentration by precipitation with GFP antibodies, a GFP-positive band of the expected size of 250 kDa was detected (Fig. 2b). A FLAG-tagged protein of about 20 kDa co-immunoprecipitated with GFP-CalS3, confirming the interaction of the two proteins. No FLAG-tagged protein was present in the precipitate of the negative control with free GFP.

Co-localisation experiments with GFP-CalS3 and RFP-RxLR3 were performed with agroinfiltrated *N. benthamiana* leaves (Fig. S6). GFP-CalS3 was expressed at low levels to confine its localisation to PD. The co-localisation experiment revealed that RFP-RxLR3 localised to the same dot-like structures as GFP-CalS3. The intensity profile confirmed the overlap of GFP and RFP signals (Fig. S6).

RxLR3 interferes with PD callose deposition and promotes cell-to-cell trafficking

The confirmation of RxLR3-CalS3 interaction raised the question if RxLR3 causes perturbation in the function of its target. The tested hypothesis was 'if presence of the effector influences deposition of callose at plasmodesmata'. The experiment with aniline blue staining revealed that, in epidermal cells of agroinfiltrated leaves of *N. benthamiana* expressing FLAG-RxLR3, the accumulation of PD callose was reduced by 37% compared with the empty vector control (Fig. S7). In line with an inhibitory function of RxLR3 on PD-localised CalS observed in *N. benthamiana*, PD callose was reduced compared with wild-type in RxLR3-expressing *Arabidopsis* lines by 37% (L2) and 43% (L3; Fig. 3). Hence, RxLR3 caused a reduction in plasmodesmal callose in both experimental systems.

The association with PD-localised CalS suggested that RxLR3 might affect plasmodesmal transport. We used the cell-to-cell spread of free GFP as a tracer in agroinfiltrated *N. benthamiana* leaves as a measure of PD conductivity (Zambryski, 2004;

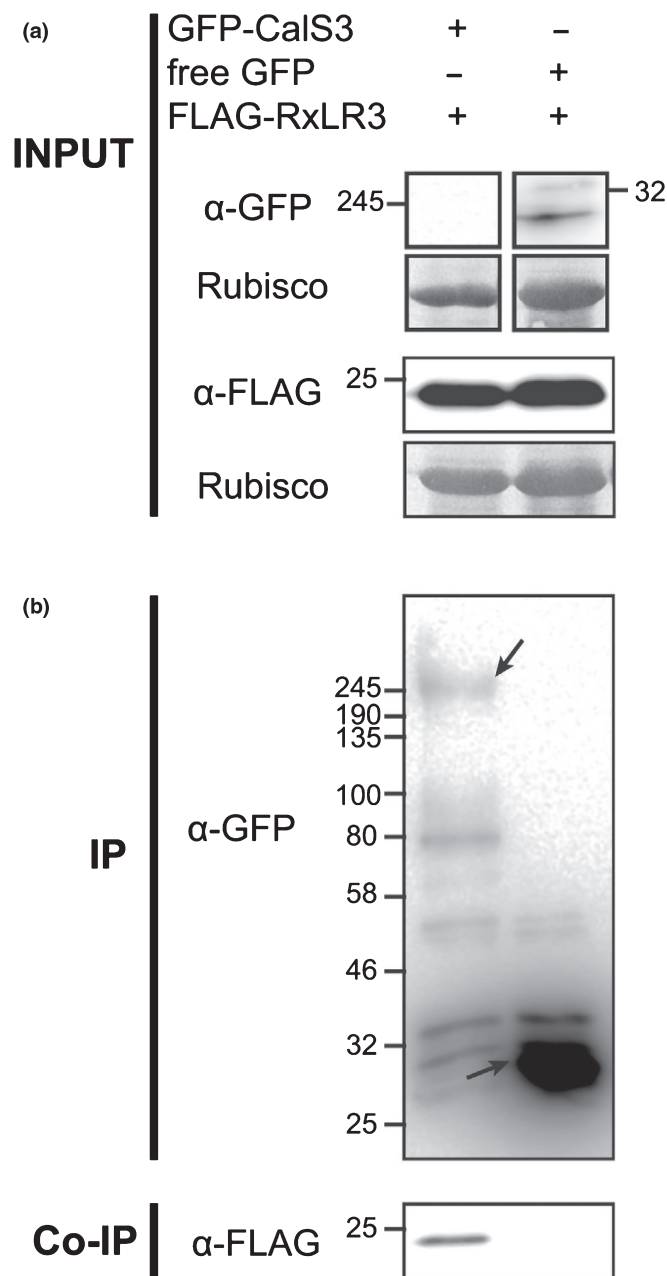


Fig. 2 Targeted co-immunoprecipitation (Co-IP) demonstrating the interaction between CalS3 and RxLR3. (a) Input used for the assays are protein extracts of *Nicotiana benthamiana* leaves co-expressing FLAG-RxLR3 together with either GFP-CalS3 or free GFP. Levels of GFP-CalS3 were too low to be detected in the initial extract. (b) Co-IP of FLAG-RxLR3 by immunoprecipitation of GFP-CalS3. Immunoprecipitation (IP) was performed using anti-GFP antibodies (α -GFP). Arrows mark bands representing the baits GFP-CalS3 (253 kDa) and free GFP (27 kDa). Presence of FLAG-RxLR3 in co-immunoprecipitates was detected with anti-FLAG antibodies (α -FLAG).

Stonebloom *et al.*, 2009). A CFP construct containing an ER-retention signal was co-transformed into agrobacteria together with free GFP as a mobile tracer. After agroinfiltration, the CFP signal marked the transformed cells and the GFP signal in the absence of CFP marked cells into which GFP had spread. Different agrobacteria concentrations were first tested for transformation

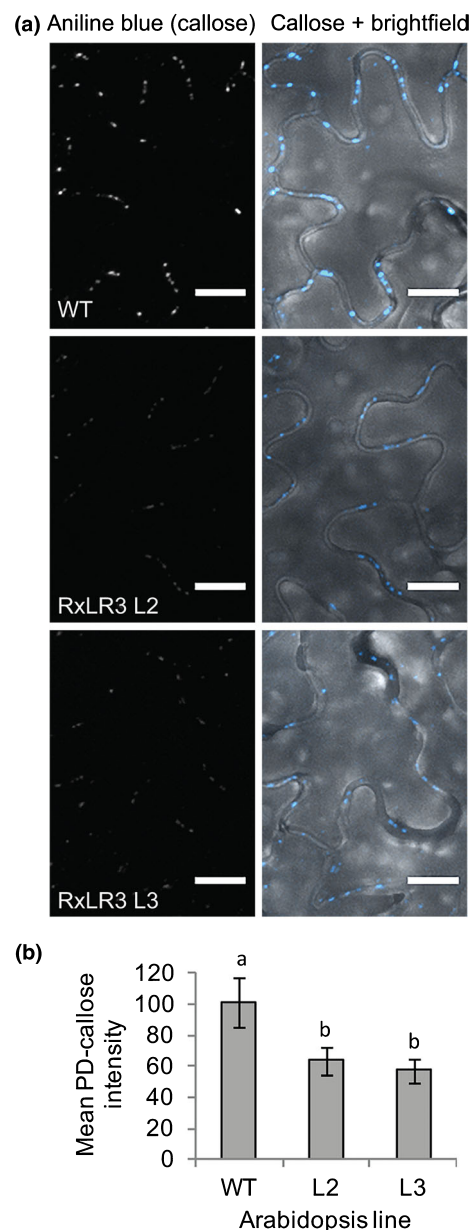


Fig. 3 Arabidopsis lines expressing RxLR3 show reduced plasmodesmata (PD) callose accumulation. (a) Callose stained with aniline blue in control plants (wild-type) and two independent transgenic lines expressing FLAG-RxLR3 (RxLR3 L2 and RxLR3 L3). Fluorescent signals represent plasmodesmal callose deposits. The panel on the left shows originally collected callose intensity that was quantified. In the right brightfield panel, callose intensity is artificially elevated to increase visibility of PD localisation on a brightfield background. Each photograph represents a z-stack consisting of 11 images with 1 μ m voxel depth. Bars, 10 μ m. (b) Quantification of signal intensity of aniline blue staining. Signal intensity of control plants was set at 100. Bars represent the mean values (\pm SE). Calculations are based on 42 photographs taken at random places in two independent experiments. Statistically significant differences are labelled as a and b based on analysis of variance (ANOVA) followed by Tukey honest significant difference (HSD) test ($P < 0.05$).

efficiency in *N. benthamiana* leaves to achieve expression of FLAG-RxLR3 in large areas (to ensure that all cells will be affected by RxLR3 presence) and expression of GFP tracer and

ER-CFP restricted to single cells (single foci/single transformation event). The effect of the concentration of the agrobacteria suspension on transformation efficiency is shown in Fig. S8. Agroinfiltration experiments were performed with an *Agrobacterium* suspension of an OD₆₀₀ of 0.15 for FLAG-RxLR3 and with a 300-times lower OD₆₀₀ of 0.0005 for agrobacteria co-expressing GFP and ER-CFP. In the absence of RxLR3, the CFP and the GFP fluorescences co-localised to the transformed epidermal cells with only weak GFP signals leaking into adjacent cells (Fig. 4a). However, in the presence of RxLR3, the GFP tracer signal spread well beyond the initially transformed cells into several layers of neighbouring cells, indicating that RxLR3 positively affected cell-to-cell movement of GFP (Fig. 4b). Quantitative analysis, performed as explained in Fig. S9, showed that in control tissue the GFP signal remained restricted to the transformed cells or to the immediate adjacent cells (transport distance ≤ 1 , 90% of observed foci) (Fig. 4a,e), whereas the spread of the GFP tracer beyond two cell layers was rarely observed. By contrast, in tissue expressing RxLR3, the GFP tracer spread beyond three layers of adjacent cells in 83% of the analysed transformation sites (foci) (Fig. 4b,e). This result is in line with the conclusion that RxLR3 has a positive effect on the cell-to-cell movement of free GFP.

To demonstrate a link between improved RxLR3-mediated GFP cell-to-cell passage and PD we took advantage of the fact that SA is known to cause closure of PD (Wang *et al.*, 2013). The experiments described above were repeated with *N. benthamiana* plants treated with SA. SA treatment strongly reduced the spread of GFP into neighbouring cells both in control tissue (Fig. 4c) and in tissue expressing RxLR3 (Fig. 4d). Quantitative analysis confirmed the inhibitory action of SA on the spread of the GFP tracer (Fig. 4e). Together, our results suggested that RxLR3 functions as a negative regulator of PD-localised CalS and as a positive regulator of PD conductivity.

RxLR3 interferes with pathogen-induced plasmodesmal callose deposition

PD callose deposition in response to *P. brassicae* was analysed in wild-type and in two transgenic RxLR3 expressing Arabidopsis lines (as described in Figs S10, S11). In response to penetration by germinating cysts of *P. brassicae*, epidermal cells of wild-type plants accumulated large deposits of callose in papillae forming at penetration sites. In addition, numerous callose deposits lining the cell periphery were formed and were consistent with a PD localisation (Fig. 5a). In contrast with wild-type plants, invaded cells of the RxLR3 lines accumulated PD callose less frequently. Quantitative analysis showed that, in wild-type plants, 90% of the invaded cells showed enhanced PD callose deposition, whereas this number was reduced to 20% and 18% in the RxLR3 lines L2 and L3, respectively (Fig. 5c).

Discussion

Our results showed that the RxLR3 effector of the Arabidopsis pathogen *P. brassicae* physically interacts with a subgroup of CalS

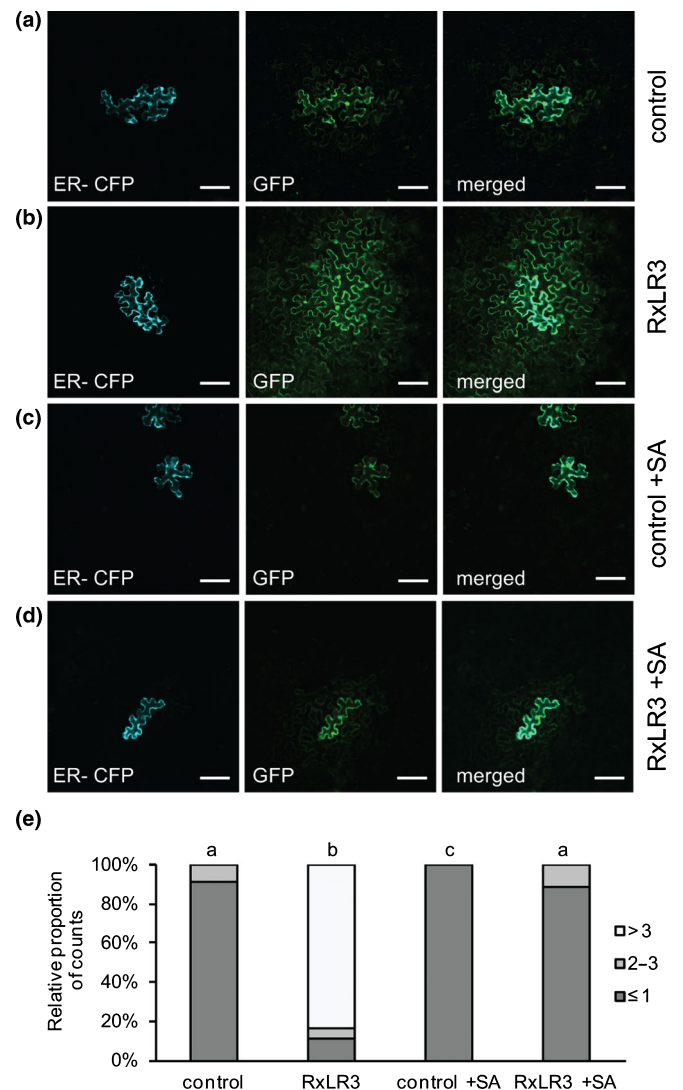


Fig. 4 RxLR3 increases cell-to-cell conductivity. Leaves of *Nicotiana benthamiana* were co-infiltrated with ER-CFP containing an ER-retention signal and free GFP as a mobile tracer together with either vector control (a) or with RxLR3 (b). Infiltration with agrobacteria containing the ER-CFP and GFP construct was performed with a low density of OD₆₀₀ 0.0005 to achieve expression in a few cells. Infiltration of agrobacteria containing a FLAG-RxLR3 construct was performed with a high density of OD₆₀₀ = 0.15 for expression in large areas of the epidermis. (c, d) Cell-to-cell movement of a GFP tracer in leaves treated with 5 mM salicylic acid (SA). Representative photographs taken with an sCMOS camera are shown. Bars, 100 μ m. (e) Quantitative analysis of GFP tracer cell-to-cell movement (see Supporting Information Fig. S9 for explanation). Results presented as relative percentage of foci (cells with single transformation event) that showed the transport distance (number of cell layers of GFP spreading) defined in the legend. Statistically significant differences labelled as a, b, c are based on multiple pairwise comparison using Fisher's exact test ($P < 0.001$; P -values adjusted for multiple testing by Benjamini–Hochberg correction). Results are based on two independent experiments with a total number of foci per treatment of $n = 176$ (considered as 100% for each bar).

that includes enzymes associated with PD. The binding of RxLR3 to these callose synthases had a negative effect on PD callose deposition in line with the conclusion that RxLR3 acts as a

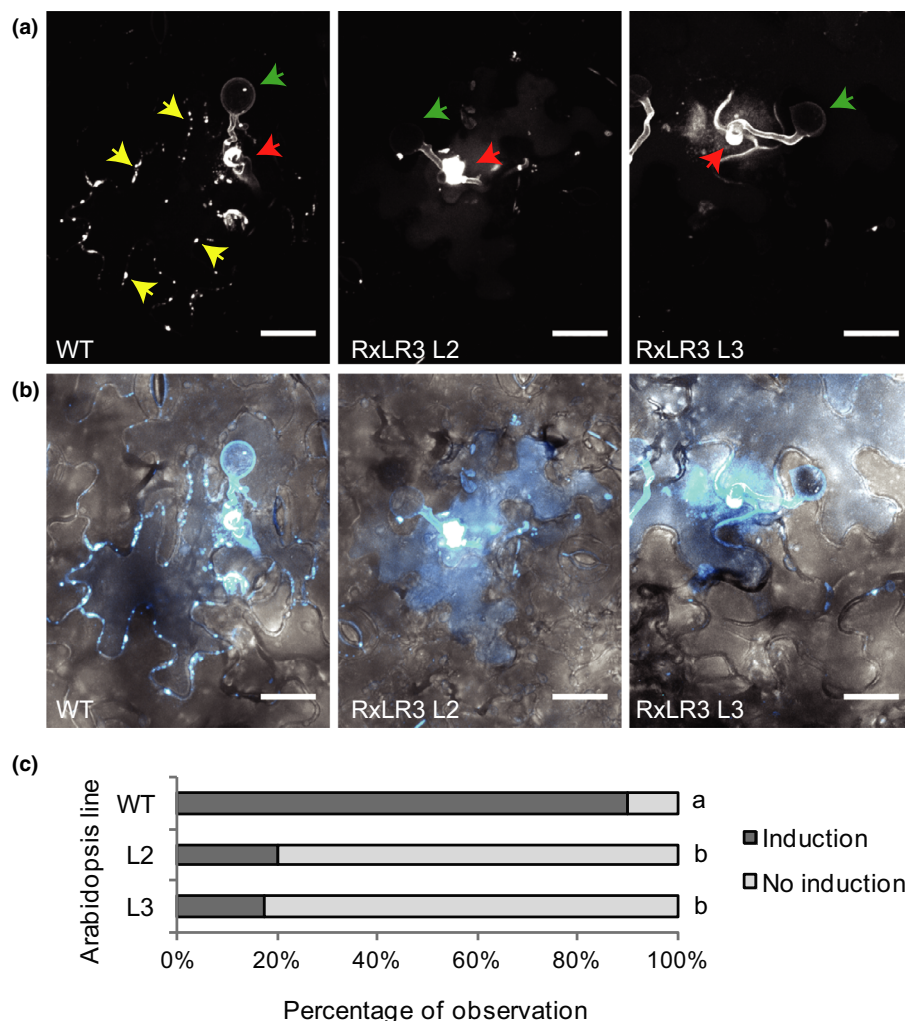


Fig. 5 RxLR3 suppresses pathogen-induced callose depositions at plasmodesmata (PD). (a) Aniline blue-stained callose depositions in Arabidopsis plants (wild-type and two independent transgenic RxLR3 lines) 7 h after inoculation with a zoospore suspension of *Phytophthora brassicae*. Germinated cysts penetrating an epidermal cell are marked with green arrows. Examples of callose deposition at PD are marked with yellow arrows and deposition of CalS12/PMR4-dependent callose in papillae formed at the site of attempted penetration are marked with red arrows. Photographs are z-stack images consisting of 17 (wild-type), 15 (RxLR3 L2) and 26 (RxLR3 L3) images were taken with an electron multiplying charge coupled device (EMCCD) camera and $\times 60$ magnification lens. All z-stack images were prepared with maximal projection type, voxel depth 1 μm . Bars, 20 μm . (b) Merged photographs showing photographs from (a) on the brightfield background. (c) Quantification of callose induction events at PD in cells attacked by germinating cysts of *P. brassicae*. Numbers of callose induction events are based on a comparison of callose staining in attacked cells versus neighbouring cells. Number of observed infection sites per genotype was $n = 40$ (see the Materials and Methods section and Supporting Information Figs S10 and S11 for further explanations). Statistically significant differences are labelled as a and b based on multiple pairwise comparison using Fisher's exact test ($P < 0.001$; P -values were adjusted for multiple testing by Benjamini–Hochberg correction).

negative regulator of PD-localised CalS-dependent callose production. The reduction of callose correlated with an enhanced PD cell-to-cell conductivity. Hence, RxLR3 is a positive regulator of PD opening, suggesting that improved cell-to-cell connectivity favours *Phytophthora* invasion of the host. Our conclusions are based on several lines of experimental evidence. First, RxLR3 localises to PD, as shown by co-localisation with the PD markers callose, PDL5 and CalS3. Second, untargeted co-immunoprecipitation followed by mass spectrometry identified the closely related callose synthases CalS1, CalS2 and CalS3 as the three top hits in the list of putative RxLR3 interaction partners, whereas none of three other tested RxLR proteins interacted with callose synthases. The interaction of CalS3 with RxLR3 was confirmed by reciprocal co-immunoprecipitation. Third, RxLR3 expression in agroinfiltrated *N. benthamiana* and in transgenic RxLR3 expressing Arabidopsis lines caused a reduction in PD callose. Fourth, RxLR3 expression enhanced cell connectivity, as shown by the accelerated cell-to-cell spread of a GFP tracer. The improved connectivity appears to be mediated by PD, as high concentrations of exogenous SA, which is known to trigger plugging of PD with callose (Zavaliev & Epel, 2015), could override the positive effect of RxLR3 on cell-to cell connectivity.

Callose deposition catalysed by CalS and callose removal catalysed by β -1,3-glucanases are mechanisms that control the aperture of PD and trafficking efficiency (Yan *et al.*, 2019). The Arabidopsis genome encodes 12 callose synthases (CalS; Verma & Hong, 2001), also referred to as GLUCAN SYNTHASE-LIKE (GSL) proteins (Zavaliev *et al.*, 2011). CalS genes encode large proteins of *c.* 250 kDa that possess multiple transmembrane domains (Hong *et al.*, 2001; Dong *et al.*, 2005; Nedukha, 2015). Individual CalS have specific functions at different subcellular locations and are differentially regulated at the transcriptional and posttranslational level in response to developmental and environmental cues (Verma & Hong, 2001; Dong *et al.*, 2008; Yu *et al.*, 2016). CalS1 (GSL6), CalS3 (GSL12), CalS8 (GSL4) and CalS10 (GSL8) were shown to be associated with PD, whereas CalS7 (GSL7) localises to PD-related phloem sieve pores (Guseman *et al.*, 2010; Vatén *et al.*, 2011; Xie & Hong, 2011; Seville *et al.*, 2013; Han *et al.*, 2014; Cui & Lee, 2016). The subcellular localisation of CalS2 has not been determined but the restricted localisation of CalS2-interacting RxLR3 to PD is suggestive of a PD localisation of CalS2.

Mature RxLR3 does not contain any targeting signals and most likely localises to PD, based on its association with CalS

enzymes. Our results demonstrated that RxLR3 interacts with CalS1, CalS2 and CalS3, which belong to a distinct subgroup CalS enzymes that shares more than 74% amino acid sequence identity. No peptide that exclusively matched to other CalS enzymes was present in the RxLR3-FLAG co-immunoprecipitate. Analysis of CalS–promoter–GUS fusions revealed that 10 out of the 12 CalS enzymes are expressed in leaves of Arabidopsis plants (Dong *et al.*, 2008). Hence, we concluded that RxLR3 interaction is most likely specific for CalS1, CalS2 and CalS3.

Our results are very compatible with an inhibitory role of RxLR3 on a subgroup of PD-localised CalS enzymes. Hence, with the production of RxLR3 *P. brassicae* tries to interfere with host-mediated closure of PD. The closure of PD via callose deposition is integrated into the innate immune system of plants (Cheval & Faulkner, 2018). Similar to local callose deposition in papillae, callose deposition at PD is triggered by the recognition of conserved microbe-associated molecular patterns and downstream SA accumulation and SA signalling via NPR1 (NONEXPRESSOR OF PR GENES 1) are critical for PD closure during defence (Wang *et al.*, 2013; Sager & Lee, 2014). It is formally not proven that SA-mediated signalling and RxLR3 affect the same CalS enzymes. SA signalling might upregulate other PD CalS enzymes such as CalS8 and CalS10, which are absent from our Co-IP list. However, within the group of callose synthases only the expression of CalS1 was strongly induced by SA (Dong *et al.*, 2008). The exact mechanism of SA-mediated closure of PD is unknown, but might depend on PD-localised PDLP and calmodulin-like proteins (Thomas *et al.*, 2008). PDLP5 was identified as an inhibitor of PD trafficking through positive modulation of callose deposition (Lee *et al.*, 2011). Interestingly, expression of PDLP5 is upregulated by SA, suggesting that closure of PD in response to SA is mediated by PDLP5-dependent activation of CalS enzymes (Wang *et al.*, 2013). A closer examination of stress-induced callose deposition using a series of Arabidopsis mutants individually targeting the 12 CalS enzymes identified CalS1 as the major callose synthase catalysing SA- and PDLP5-dependent PD callose production (Cui & Lee, 2016). Hence, SA signalling and RxLR3 both target CalS1 and compete for its functional control.

Pathogen-induced accumulation of SA is a hallmark of nearly all plant–pathogen interactions including the Arabidopsis–*P. brassicae* interaction (Roetschi *et al.*, 2001) and *Agrobacterium* challenged tobacco plants (Lee *et al.*, 2009). However, PD closure in response to pathogens other than viruses has received little attention (Benhamou & Côté, 1992; Giesbrecht *et al.*, 2011). Plants defective in PD closure were shown to be more susceptible to disease (Lee *et al.*, 2011; Faulkner *et al.*, 2013). Our results showed that inoculation of Arabidopsis plants with *P. brassicae* triggered callose depositions at the PD of infected cells. Arabidopsis accession Ws-0 is resistant to the *P. brassicae* isolate CBS 179.87 and, apparently, it wins the battle for control of PD connectivity. However, the frequency of pathogen-induced accumulation of PD callose was much reduced in transgenic RxLR3 lines indicating that, depending on the level, RxLR3 is competitive in preventing PD callose depositions in inoculated plants. The Arabidopsis lines with constitutive RxLR3 expression were smaller

and showed enhanced symptom development compared with the wild-type. Whether the disease resistance phenotype is caused by enhanced PD conductivity or is the result of growth-related secondary effects remains to be shown. Single effectors are not expected to have a major effect on disease resistance of Arabidopsis towards *P. brassicae*, as resistance depends on the combinatorial activity of different defence responses (Schlaeppli *et al.*, 2010).

The reasons why host plants upon inoculation aim to close PD and pathogens try to open PD are comprehensible at local infection sites. However, the closure of PD in response to SA is counterintuitive for SAR that depends on PD-mediated trafficking of signalling molecules and DIR1 (DEFECTIVE IN INDUCED RESISTANCE1), a lipid transfer protein proposed to escort some SAR signals via PD and phloem to systemic leaves (Carella *et al.*, 2015; Lim *et al.*, 2016). With respect to SAR the function of RxLR3 as a promoter of PD trafficking is equally counterintuitive, as RxLR3 is expected to boost cell-to-cell movement of SAR signals. These contradicting activities might be resolved in the future by analysing infected host cells for comparative kinetics of SA accumulation, RxLR3 delivery into host cells, PD conductance and SAR signalling. There is evidence that SAR signalling molecules move out from infected cells before SA-mediated PD callose deposition occurs (Carella *et al.*, 2015; Lim *et al.*, 2016).

Some filamentous pathogens spread within the host plant via PD. The hyphae of the rice pathogen *Magnaporthe oryzae* use PD to cross plant cell walls and grow from cell to cell (Kankanala *et al.*, 2007). The idea of PD as natural gates for hyphal growth into neighbouring cells was also reported for *Phytophthora ramorum* (Giesbrecht *et al.*, 2011). Interestingly, *M. oryzae* delivers effector proteins from colonised cells via PD into adjacent uninfected cells, presumably to pre-emptively suppress resistance responses (Khang *et al.*, 2010). Cell-to-cell movement was also demonstrated for the Cmu1 effector of the maize pathogen *Ustilago maydis* (Djamei *et al.*, 2011). Cmu1 encodes a chorismate mutase that interferes with the production of SA, suggesting a function of Cmu1 in suppression of SA-mediated defence responses in advance of the pathogen. It is expected that effectors, such as RxLR3, that positively regulate PD connectivity will promote the cell-to-cell movement of other effectors and thereby potentiate their impact. For example, the Six5/Avr2 effector pair of *Fusarium oxysporum* alters PD permeability by an unknown mechanism to facilitate cell-to-cell movement of the effector Avr2 (Cao *et al.*, 2018) and the MLP37347 candidate effector from the poplar rust fungus *Melampsora larici-populina* is associated with PD but its host target and effect on PD permeability were not analysed (Germain *et al.*, 2018). Similar to RxLR3, the HopO1-1 effector of bacterial pathogen *Pseudomonas syringae* also increased the distance of PD-dependent transport. Its interaction with PDLP7 and PDLP5 led to destabilisation of these two targets and, as a result, there was enhanced pathogen spread to neighbouring tissues (Aung *et al.*, 2019).

One interesting aspect to investigate in the future would be to dissect elements of intercellular PD channels occupied by these pathogen effectors. Our co-localisation study of RxLR3 and PDLP5 showed that spatial distance between them reached *c.* 500 nm. It has also been shown previously that the PDLP5

localisation pattern did not completely overlap with *Tobacco mosaic virus* (TMV) movement protein (MP), despite the fact that both proteins are PD localised (Lee *et al.*, 2011).

Together, our results add further evidence that PD are an important battle ground in plant–pathogen interactions that are targeted by viral, fungal and oomycete effectors as well as by host-mediated SA signalling. Whether the host plant or the pathogen gains control depends on the respective kinetics and strength of cellular effector and SA accumulation. Especially when combined with effectors targeting SA signalling, effectors with a negative impact on PD gating, such as RxLR3, are expected to enhance the cell-to-cell distribution of signalling molecules and nutritional compounds.

Accession numbers

RxLR3: GenBank MN708974.

RxLR5: GenBank MN708975.

RxLR19: GenBank MN708976.

RxLR29: GenBank MG489829.

Acknowledgements


The authors are thankful to Boris Egger, University of Fribourg, Switzerland, for technical help and advice with confocal microscopy. We thank Kyaw Joe Aung, Iowa State University, USA, for his advice and sharing the ER-CFP construct, and Ykä Helariutta, University of Helsinki, Finland, for providing the GFP-CalS3 construct. LC-MS/MS analysis was performed by the Protein Analysis Facility of the Center for Integrative Genomics, University of Lausanne, Switzerland. We thank Thierry Laroche (BioImaging and Optics Core Facility, EPFL, Lausanne) for his help in high resolution microscopy. The project was supported by the Swiss National Science Foundation (31003A 129696 and P2FRP3_188054).

Author contributions

IT, MS and FM planned and designed the research. MS produced transgenic plants and conducted untargeted Co-IP. TGD contributed to the reciprocal Co-IP experiment and cloning. IT performed all agroinfiltration experiments, confocal microscopy and the analysis of PD conductivity. IT and FM wrote the manuscript.

ORCID

Felix Mauch  <https://orcid.org/0000-0001-5150-2711>

Iga Tomczynska  <https://orcid.org/0000-0002-3413-5670>

References

- Amsbury S, Kirk P, Benitez-Alfonso Y. 2017. Emerging models on the regulation of intercellular transport by plasmodesmata-associated callose. *Journal of Experimental Botany* **69**: 105–115.
- Anderson RG, Deb D, Fedkenheuer K, McDowell JM. 2015. Recent progress in RXLR effector research. *Molecular Plant–Microbe Interactions* **28**: 1063–1072.
- Aung K, Kim P, Li Z, Joe A, Kvitko BH, Alfano JR, He SY. 2019. Pathogenic bacteria target plant plasmodesmata to colonize and invade surrounding tissues. *Plant Cell* **32**: 595–611.
- Bayer EMF, Salmon MS. 2013. Dissecting plasmodesmata molecular composition by mass spectrometry-based proteomics. *Frontiers in Plant Science* **3**: 307.
- Benhamou N, Côté F. 1992. Ultrastructure and cytochemistry of pectin and cellulose degradation in tobacco roots infected by *Phytophthora parasitica* var. *nicotianae*. *Phytopathology* **82**: 468–478.
- Benitez-Alfonso Y, Faulkner C, Pendle A, Miyashima S, Helariutta Y, Maule A. 2013. Symplastic intercellular connectivity regulates lateral root patterning. *Developmental Cell* **26**: 136–147.
- Benitez-Alfonso Y, Faulkner C, Ritzenthaler C, Maule AJ. 2010. Plasmodesmata: gateways to local and systemic virus infection. *Molecular Plant–Microbe Interactions* **23**: 1403–1412.
- Burch-Smith TM, Zambryski PC. 2010. Loss of INCREASED SIZE EXCLUSION LIMIT (ISE) 1 or ISE2 increases the formation of secondary plasmodesmata. *Current Biology* **20**: 989–993.
- Cao L, Blekemolen MC, Tintor N, Cornelissen BJ, Takken FL. 2018. The *Fusarium oxysporum* Avr2-Six5 effector pair alters plasmodesmatal exclusion selectivity to facilitate cell-to-cell movement of Avr2. *Molecular Plant* **11**: 691–705.
- Carella P, Isaacs M, Cameron R. 2015. Plasmodesmata-located protein overexpression negatively impacts the manifestation of systemic acquired resistance and the long-distance movement of defective induced resistance1 in *Arabidopsis*. *Plant Biology* **17**: 395–401.
- Chaparro-Garcia A, Schwizer S, Sklenar J, Yoshida K, Petre B, Bos JJ, Schornack S, Jones AM, Bozkurt TO, Kamoun S. 2015. *Phytophthora infestans* RXLR-WY effector AVR3a associates with dynamin-related protein 2 required for endocytosis of the plant pattern recognition receptor FLS2. *PLoS ONE* **10**: e0137071.
- Chen X-Y, Kim J-Y. 2009. Callose synthesis in higher plants. *Plant Signaling & Behavior* **4**: 489–492.
- Cheval C, Faulkner C. 2018. Plasmodesmal regulation during plant–pathogen interactions. *New Phytologist* **217**: 62–67.
- Clough SJ, Bent AF. 1998. Floral dip: a simplified method for *Agrobacterium*-mediated transformation of *Arabidopsis thaliana*. *The Plant Journal* **16**: 735–743.
- Cui W, Lee J-Y. 2016. *Arabidopsis* callose synthases CalS1/8 regulate plasmodesmal permeability during stress. *Nature Plants* **2**: 16034.
- Dagdas YF, Belhaj K, Maqbool A, Chaparro-Garcia A, Pandey P, Petre B, Tabassum N, Cruz-Mireles N, Hughes RK, Sklenar J *et al.* 2016. An effector of the Irish potato famine pathogen antagonizes a host autophagy cargo receptor. *eLife* **5**: e10856.
- De Storme N, Geelen D. 2014. Callose homeostasis at plasmodesmata: molecular regulators and developmental relevance. *Frontiers in Plant Science* **5**: 138.
- Djamei A, Schipper K, Rabe F, Ghosh A, Vincon V, Kahnt J, Osorio S, Tohge T, Fernie AR, Feussner I. 2011. Metabolic priming by a secreted fungal effector. *Nature* **478**: 395.
- Dong X, Hong Z, Chatterjee J, Kim S, Verma DPS. 2008. Expression of callose synthase genes and its connection with Npr1 signaling pathway during pathogen infection. *Planta* **229**: 87–98.
- Dong X, Hong Z, Sivaramakrishnan M, Mahfouz M, Verma DPS. 2005. Callose synthase (CalS5) is required for exine formation during microgametogenesis and for pollen viability in *Arabidopsis*. *The Plant Journal* **42**: 315–328.
- Du Y, Mpina MH, Birch PR, Bouwmeester K, Govers F. 2015. *Phytophthora infestans* RXLR effector AVR1 interacts with exocyst component Sec5 to manipulate plant immunity. *Plant Physiology* **169**: 1975–1990.
- Fan G, Yang Y, Li T, Lu W, Du Y, Qiang X, Wen Q, Shan W. 2018. A *Phytophthora capsici* RXLR effector targets and inhibits a plant PPIase to suppress endoplasmic reticulum-mediated immunity. *Molecular Plant* **11**: 1067–1083.
- Faulkner C, Maule A. 2011. Opportunities and successes in the search for plasmodesmal proteins. *Protoplasma* **248**: 27–38.

- Faulkner C, Petutschnig E, Benitez-Alfonso Y, Beck M, Robatzek S, Lipka V, Maule AJ. 2013. LYM2-dependent chitin perception limits molecular flux via plasmodesmata. *Proceedings of the National Academy of Sciences, USA* 110: 9166–9170.
- Fernandez-Calvino L, Faulkner C, Walshaw J, Saalbach G, Bayer E, Benitez-Alfonso Y, Maule A. 2011. Arabidopsis plasmodesmal proteome. *PLoS ONE* 6: e18880.
- Gaudioso-Pedraza R, Benitez-Alfonso Y. 2014. A phylogenetic approach to study the origin and evolution of plasmodesmata-localized glycosyl hydrolases family 17. *Frontiers in Plant Science* 5: 212.
- Germain H, Joly DL, Mireault C, Plourde MB, Letanneur C, Stewart D, Morency MJ, Petre B, Duplessis S, Séguin A. 2018. Infection assays in Arabidopsis reveal candidate effectors from the poplar rust fungus that promote susceptibility to bacteria and oomycete pathogens. *Molecular Plant Pathology* 19: 191–200.
- Giesbrecht MB, Hansen EM, Kitin P. 2011. Histology of *Phytophthora ramorum* in *Notholithocarpus densiflorus* bark tissues. *New Zealand Journal of Forestry Science* 41: 89–100.
- Giraldo MC, Valent B. 2013. Filamentous plant pathogen effectors in action. *Nature Reviews Microbiology* 11: 800–814.
- Grisson MS, Brocard L, Fouillen L, Nicolas W, Wewer V, Dörmann P, Nacir H, Benitez-Alfonso Y, Claverol S, Germain V. 2015. Specific membrane lipid composition is important for plasmodesmata function in Arabidopsis. *Plant Cell* 27: 1228–1250.
- Gunning BE, Robards A. 1976. *Intercellular communication in plants: studies on plasmodesmata*. Berlin, Germany: Springer-Verlag.
- Guseman JM, Lee JS, Bogenschutz NL, Peterson KM, Virata RE, Xie B, Kanaoka MM, Hong Z, Torii KU. 2010. Dysregulation of cell-to-cell connectivity and stomatal patterning by loss-of-function mutation in Arabidopsis choroid (glucan synthase-like 8). *Development* 137: 1731–1741.
- Haas BJ, Kamoun S, Zody MC, Jiang RH, Handsaker RE, Cano LM, Grabherr M, Kodira CD, Raffaele S, Torto-Alalibo T. 2009. Genome sequence and analysis of the Irish potato famine pathogen *Phytophthora infestans*. *Nature* 461: 393–398.
- Han X, Hyun TK, Zhang M, Kumar R, Koh E-j, Kang B-H, Lucas WJ, Kim J-Y. 2014. Auxin-callose-mediated plasmodesmal gating is essential for tropic auxin gradient formation and signaling. *Developmental Cell* 28: 132–146.
- Hong Z, Delauney AJ, Verma DPS. 2001. A cell plate-specific callose synthase and its interaction with phragmoplastin. *Plant Cell* 13: 755–768.
- Huang J, Gu L, Zhang Y, Yan T, Kong G, Kong L, Guo B, Qiu M, Wang Y, Jing M. 2017. An oomycete plant pathogen reprograms host pre-mRNA splicing to subvert immunity. *Nature Communications* 8: 2051.
- Jing M, Guo B, Li H, Yang B, Wang H, Kong G, Zhao Y, Xu H, Wang Y, Ye W. 2016. A *Phytophthora sojae* effector suppresses endoplasmic reticulum stress-mediated immunity by stabilizing plant binding immunoglobulin proteins. *Nature Communications* 7: 1–17.
- Kale SD, Gu B, Capelluto DG, Dou D, Feldman E, Rumore A, Arredondo FD, Hanlon R, Fudal I, Rouxel T. 2010. External lipid PI3P mediates entry of eukaryotic pathogen effectors into plant and animal host cells. *Cell* 142: 284–295.
- Kankanala P, Czymmek K, Valent B. 2007. Roles for rice membrane dynamics and plasmodesmata during biotrophic invasion by the blast fungus. *Plant Cell* 19: 706–724.
- Khang CH, Berruyer R, Giraldo MC, Kankanala P, Park S-Y, Czymmek K, Kang S, Valent B. 2010. Translocation of *Magnaporthe oryzae* effectors into rice cells and their subsequent cell-to-cell movement. *Plant Cell* 22: 1388–1403.
- King SR, McLellan H, Boevink PC, Armstrong MR, Bukharova T, Sukarta O, Win J, Kamoun S, Birch PR, Banfield MJ. 2014. *Phytophthora infestans* RXLR effector PexRD2 interacts with host MAPKKK epsilon to suppress plant immune signaling. *Plant Cell* 26: 1345–1359.
- Kong L, Qiu X, Kang J, Wang Y, Chen H, Huang J, Qiu M, Zhao Y, Kong G, Ma Z. 2017. A *Phytophthora* effector manipulates host histone acetylation and reprograms defense gene expression to promote infection. *Current Biology* 27: 981–991.
- Lee C-W, Efetova M, Engelmann JC, Kramell R, Wasternack C, Ludwig-Müller J, Hedrich R, Deeken R. 2009. Agrobacterium tumefaciens promotes tumor induction by modulating pathogen defense in *Arabidopsis thaliana*. *Plant Cell* 21: 2948–2962.
- Lee J-Y, Wang X, Cui W, Sager R, Modla S, Czymmek K, Zybaliov B, van Wijk K, Zhang C, Lu H. 2011. A plasmodesmata-localized protein mediates crosstalk between cell-to-cell communication and innate immunity in Arabidopsis. *Plant Cell* 23: 3353–3373.
- Lim G-H, Shine M, de Lorenzo L, Yu K, Cui W, Navarre D, Hunt AG, Lee J-Y, Kachroo A, Kachroo P. 2016. Plasmodesmata localizing proteins regulate transport and signaling during systemic acquired immunity in plants. *Cell Host & Microbe* 19: 541–549.
- Lucas WJ, Bouché-Pillon S, Jackson DP, Nguyen L, Baker L, Ding B, Hake S. 1995. Selective trafficking of KNOTTED1 homeodomain protein and its mRNA through plasmodesmata. *Science* 270: 1980–1983.
- Murphy F, He Q, Armstrong M, Giuliani LM, Boevink PC, Zhang W, Tian Z, Birch PR, Gilroy EM. 2018. Potato MAP3K StVIK is required for *Phytophthora infestans* RXLR Effector Pi17316 to promote disease. *Plant Physiology* 177: 398–410.
- Nakajima K, Sena G, Nawy T, Benfey PN. 2001. Intercellular movement of the putative transcription factor SHR in root patterning. *Nature* 413: 307.
- Nedukha O. 2015. Callose: localization, functions, and synthesis in plant cells. *Cytology and Genetics* 49: 49–57.
- Oparka KJ. 2004. Getting the message across: how do plant cells exchange macromolecular complexes? *Trends in Plant Science* 9: 33–41.
- Petre B, Kopischke M, Evrard A, Robatzek S, Kamoun S. 2016. Cell re-entry assays do not support models of pathogen-independent translocation of AvrM and AVR3a effectors into plant cells. *BioRxiv* 038232.
- Qiao Y, Shi J, Zhai Y, Hou Y, Ma W. 2015. *Phytophthora* effector targets a novel component of small RNA pathway in plants to promote infection. *Proceedings of the National Academy of Sciences, USA* 112: 5850–5855.
- Radford J, Vesik M, Overall R. 1998. Callose deposition at plasmodesmata. *Protoplasma* 201: 30–37.
- Reagan BC, Ganusov EE, Fernandez JC, McCray TN, Burch-Smith TM. 2018. RNA on the move: the plasmodesmata perspective. *Plant Science* 275: 1–10.
- Roberts A, Oparka K. 2003. Plasmodesmata and the control of symplastic transport. *Plant, Cell & Environment* 26: 103–124.
- Roetschi A, Si-Ammour A, Belbahri L, Mauch F, Mauch-Mani B. 2001. Characterization of an Arabidopsis-*Phytophthora* pathosystem: resistance requires a functional PAD2 gene and is independent of salicylic acid, ethylene and jasmonic acid signalling. *The Plant Journal* 28: 293–305.
- Sager R, Lee J-Y. 2014. Plasmodesmata in integrated cell signalling: insights from development and environmental signals and stresses. *Journal of Experimental Botany* 65: 6337–6358.
- Schlaeppli K, Abou-Mansour E, Buchala A, Mauch F. 2010. Disease resistance of Arabidopsis to *Phytophthora brassicae* is established by the sequential action of indole glucosinolates and camalexin. *The Plant Journal* 62: 840–851.
- Schütze K, Harter K, Chaban C. 2009. Bimolecular fluorescence complementation (BiFC) to study protein-protein interactions in living plant cells. In: Pfannschmidt T, ed. *Plant signal transduction. Methods in molecular biology*, vol. 479. Totowa, NJ, USA: Humana Press, 189–202.
- Sevilem I, Miyashima S, Helariutta Y. 2013. Cell-to-cell communication via plasmodesmata in vascular plants. *Cell Adhesion & Migration* 7: 27–32.
- Sevilem I, Yadav SR, Helariutta Y. 2015. Plasmodesmata: channels for intercellular signaling during plant growth and development. In: Heinlein M, ed. *Plasmodesmata: methods and protocols*. New York, NY, USA: Humana Press, 3–24.
- Shimada TL, Shimada T, Hara-Nishimura I. 2010. A rapid and non-destructive screenable marker, FAST, for identifying transformed seeds of *Arabidopsis thaliana*. *The Plant Journal* 61: 519–528.
- Stonebloom S, Burch-Smith T, Kim I, Meinke D, Mindrinos M, Zambryski P. 2009. Loss of the plant DEAD-box protein ISE1 leads to defective mitochondria and increased cell-to-cell transport via plasmodesmata. *Proceedings of the National Academy of Sciences, USA* 106: 17229–17234.
- Thomas CL, Bayer EM, Ritzenthaler C, Fernandez-Calvino L, Maule AJ. 2008. Specific targeting of a plasmodesmal protein affecting cell-to-cell communication. *PLoS Biology* 6: e7.

- Tomczynska I, Stumpe M, Mauch F. 2018. A conserved RxLR effector interacts with host RABA-type GTPases to inhibit vesicle-mediated secretion of antimicrobial proteins. *The Plant Journal* **95**: 187–203.
- Tyler BM. 2009. Entering and breaking: virulence effector proteins of oomycete plant pathogens. *Cellular Microbiology* **11**: 13–20.
- Tyler BM, Kale SD, Wang Q, Tao K, Clark HR, Drews K, Antignani V, Rumore A, Hayes T, Plett JM. 2013. Microbe-independent entry of oomycete RxLR effectors and fungal RxLR-like effectors into plant and animal cells is specific and reproducible. *Molecular Plant–Microbe Interactions* **26**: 611–616.
- Vatén A, Dettmer J, Wu S, Stierhof Y-D, Miyashima S, Yadav SR, Roberts CJ, Campilho A, Bulone V, Lichtenberger R. 2011. Callose biosynthesis regulates symplastic trafficking during root development. *Developmental Cell* **21**: 1144–1155.
- Verma DPS, Hong Z. 2001. Plant callose synthase complexes. *Plant Molecular Biology* **47**: 693–701.
- Wang X, Sager R, Cui W, Zhang C, Lu H, Lee J-Y. 2013. Salicylic acid regulates plasmodesmata closure during innate immune responses in Arabidopsis. *Plant Cell* **25**: 2315–2329.
- Wawra S, Trusch F, Matena A, Apostolakis K, Linne U, Zhukov I, Stanek J, Koźmiński W, Davidson I, Secombes CJ. 2017. The RxLR motif of the host targeting effector AVR3a of *Phytophthora infestans* is cleaved before secretion. *Plant Cell* **29**: 1184–1195.
- Whisson SC, Avrova AO, Boevink PC, Armstrong MR, Seman ZA, Hein I, Birch PRJ. 2011. Exploiting knowledge of pathogen effectors to enhance late blight resistance in potato. *Potato Research* **54**: 325–340.
- Whisson SC, Boevink PC, Moleleki L, Avrova AO, Morales JG, Gilroy EM, Armstrong MR, Grouffaud S, Van West P, Chapman S. 2007. A translocation signal for delivery of oomycete effector proteins into host plant cells. *Nature* **450**: 115.
- Xie B, Hong Z. 2011. Unplugging the callose plug from sieve pores. *Plant Signaling & Behavior* **6**: 491–493.
- Yan D, Yadav SR, Paterlini A, Nicolas WJ, Petit JD, Brocard L, Belevich I, Grison MS, Vatén A, Karami L *et al.* 2019. Sphingolipid biosynthesis modulates plasmodesmal ultrastructure and phloem unloading. *Nature Plants* **5**: 604–615.
- Yu Y, Jiao L, Fu S, Yin L, Zhang Y, Lu J. 2016. Callose synthase family genes involved in the grapevine defense response to downy mildew disease. *Phytopathology* **106**: 56–64.
- Zambryski P. 2004. Cell-to-cell transport of proteins and fluorescent tracers via plasmodesmata during plant development. *Journal of Cell Biology* **164**: 165–168.
- Zavaliev R, Epel BL. 2015. Imaging callose at plasmodesmata using aniline blue: quantitative confocal microscopy. In: Heinlein M, ed. *Plasmodesmata: Methods and Protocols*. New York, NY, USA: Springer, 105–119.
- Zavaliev R, Ueki S, Epel BL, Citovsky V. 2011. Biology of callose (β -1,3-glucan) turnover at plasmodesmata. *Protoplasma* **248**: 117–130.
- Zheng X, McLellan H, Fraiture M, Liu X, Boevink PC, Gilroy EM, Chen Y, Kandel K, Sessa G, Birch PR *et al.* 2014. Functionally redundant RXLR effectors from *Phytophthora infestans* act at different steps to suppress early flg22-triggered immunity. *PLoS Pathogens* **10**: e1004057.
- Fig. S1** Amino acid sequence of the RxLR3 effector of *P. brassicae*.
- Fig. S2** Relative *RxLR3* expression during *P. brassicae* infection.
- Fig. S3** Ectopically expressed RxLR3 interferes with Arabidopsis development.
- Fig. S4** Effect of RxLR3 expression on disease resistance towards *P. brassicae*.
- Fig. S5** GFP-RxLR3 localises to dot-like structures at the cell periphery.
- Fig. S6** RxLR3 co-localises with CalS3.
- Fig. S7** RxLR3 causes reduced callose deposition at PD in *N. benthamiana* epidermal cells.
- Fig. S8** Effect of *Agrobacterium* density on expression pattern of RxLR3 in agroinfiltrated *N. benthamiana*.
- Fig. S9** Assessment of GFP tracer diffusion assay in agroinfiltrated *N. benthamiana* epidermal cells.
- Fig. S10** The PD callose quantification method in epidermal cells of Arabidopsis wild-type and RxLR3 transgenic lines after infection with *P. brassicae* zoospores.
- Fig. S11** The overview: examples of Arabidopsis epidermal cells of (a) wild-type and (b) RxLR3 transgenic lines scored as showing ‘induced’ or ‘noninduced’ PD callose in cells invaded by *P. brassicae* zoospore.
- Table S1** List of primers.
- Table S2** List of constructs.
- Table S3** List of top candidates of RxLR3 interacting proteins identified with Co-IP/MS with FLAG-RxLR3 as a bait.

Please note: Wiley Blackwell are not responsible for the content or functionality of any Supporting Information supplied by the authors. Any queries (other than missing material) should be directed to the *New Phytologist* Central Office.

Supporting Information

Additional Supporting Information may be found online in the Supporting Information section at the end of the article.